Oxygen-activated epitaxial recrystallization of Li-implanted α-SiO_2

M. Gustafsson
Accelerator Laboratory, University of Helsinki, P.O. Box 43, FIN-00014 Helsinki, Finland

F. Roccaforte
II. Physikalisches Institut and Sonderforschungsberiech 345, Universität Göttingen, Bunsenstrasse 7-9, D-37073 Göttingen, Germany

J. Keinonen
Accelerator Laboratory, University of Helsinki, P.O. Box 43, FIN-00014 Helsinki, Finland
and II. Physikalisches Institut and Sonderforschungsberiech 345, Universität Göttingen, Bunsenstrasse 7-9, D-37073, Göttingen, Germany

W. Bolse
II. Physikalisches Institut and Sonderforschungsberiech 345, Universität Göttingen, Bunsenstrasse 7-9, D-37073 Göttingen Germany
and Institut für Strahlenphysik, Universität Stuttgart, Allmandring 3, D-70569 Stuttgart, Germany

L. Ziegeler
II. Physikalisches Institut and Sonderforschungsberiech 345, Universität Göttingen, Bunsenstrasse 7-9, D-37073 Göttingen, Germany

K. P. Lieb
II. Physikalisches Institut and Sonderforschungsberiech 345, Universität Göttingen, Bunsenstrasse 7-9, D-37073 Göttingen, Germany
(Received 15 July 1999)

A very strong exchange of oxygen between α-quartz (^{16}O) and annealing atmosphere (^{18}O) observed during solid-phase epitaxial growth of Li^+- and Cs^+-ion-beam-amorphized single-crystal α-quartz is reported. Epitaxial regrowth was observed in Li-irradiated samples after 700 °C annealing and in Cs-irradiated samples after 870 °C annealing, by means of Rutherford backscattering spectrometry in channeling geometry. The $^{18}O/^{16}O$ exchange and the outdiffusion of Li were investigated by the use of time-of-flight elastic recoil detection analysis. Our experiments show that alkali-ion implantation strongly enhances the exchange of ^{16}O in SiO_2 with ^{18}O of the annealing atmosphere. The exchange accompanies the loss of alkali atoms, thus favoring the recrystallization of the lattice. Mechanisms of epitaxial regrowth in Li- and Cs-implanted α-quartz are discussed.

I. INTRODUCTION

Crystalline α-quartz and amorphous SiO_2(a-SiO_2) offer a wide range of technological applications and represent one of the most important dielectric in microelectronics[1,2] and optoelectronic device technology.[3] Manifold applications of those materials can be found, for example, in optical waveguides, switches, and amplifiers. For processing of α-quartz and a-SiO_2 the ion beam is an indispensable tool. However, ion irradiation of α-quartz leads to aperiodic (highly damaged or amorphized) networks already at low ion fluences. Much effort has been devoted in the last two decades to understand the mechanisms of the disordering of SiO_2 by ion irradiation, the stability of the defects, and the solid-phase epitaxial growth (SPEG) of ion-beam-amorphized layers.[3–23]

Although many attempts were made, complete annealing of defects in ion-irradiated SiO_2 films was not achieved below 1200 °C until recently.[11–14] SPEG of ion-beam amorphized α-quartz upon thermal annealing was therefore ruled out both from experimental results[15] and theoretical considerations.[16] Very recently, Roccaforte *et al.*[20–22] observed epitaxial recrystallization of ion-irradiated α-quartz after alkali implantation and annealing in air. They found that SPEG of Cs-implanted α-quartz occurs at 875 °C when annealing in air, while only very little regrowth takes place in vacuum. On the other hand, after implantation of self-ions (namely, stoichiometric amounts of Si^+ and O^+ ions) or Xe^+ ions, no epitaxial recrystallization was observed up to temperatures of about 900 °C.

The influence of alkali ions and annealing environments was explained in terms of topological alterations in the [SiO_4]-tetrahedral network.[20–23] The implantation of Cs ions and subsequent annealing in air were suggested to result in the formation of Cs_2O network modifier. The alkali oxide dissolved inside the SiO_2 amorphous network breaks up the corner-sharing [SiO_4]-tetrahedral network by generating nonconnected tetrahedron corners,[24] but leaves the [SiO_4] tetrahedra intact. This reduces the average connectivity of the amorphous network and thus increases its recrystallization probability.

To understand in more detail the role of oxygen and damage produced during ion irradiation, we have studied in the current work SPEG in Li- and Cs-implanted samples annealed in an ^{18}O atmosphere. The migration of ^{16}O out of the sample and ^{18}O into the sample was observed by the time-of-flight elastic recoil detection analysis (TOF-ERDA) technique. Our experiments show that the alkali-irradiation-

induced damage enhances the outdiffusion of ^{16}O and indiffusion of ^{18}O, giving rise to a strong exchange of the oxygen isotopes in the damaged region. This exchange accompanies the loss of alkali atoms and favors the epitaxial recrystallization of the lattice. For this kind of investigation, a combination of depth profiling methods [Rutherford backscattering spectrometry (RBS), TOF-ERDA] of all relevant elements and isotopes and RBS channeling for probing the crystallinity of the bulk surface layer was used.

II. EXPERIMENT

Single-crystalline (0001) α-quartz samples, 10 mm $\times$10 mm in area and 1 mm thick, were irradiated with 15-keV Li^+ or 250-keV Cs^+ ions to a fluence of 2.5×10^{16} ions/cm^2, using the Göttingen heavy ion implanter IONAS.[25] For comparison of oxygen migration, samples of 2.5×10^{16} 250-keV Xe^+ ions/cm^2 were also prepared. The energies were chosen to obtain the same projected range in all the implantations, as predicted by TRIM95 calculations.[26] During irradiation the samples were kept in thermal contact to a liquid nitrogen reservoir (77 K). The beam heating of a sample was avoided by keeping the ion-beam current below 2 μA. The ion beam was swept over the sample surface by means of an electric *x-y* sweep system in order to achieve a homogeneous implantation. The *c* axes of the samples were misaligned by 6° with respect to the beam direction to prevent channeling of the impinging ions.

After implantation, 1 h isochronal thermal annealing of the samples was carried out in an ^{18}O atmosphere and air at temperatures between 300 and 800°C. For annealing in ^{18}O, the sample was put into a quartz glass ampoule. After having evacuated the ampoule to about 4×10^{-5} mbar, the glass tube was filled with enriched (98%) ^{18}O gas at a pressure required to have 1 atm at a wanted annealing temperature. Then the sample was encapsulated by melting the top of the ampoule, and the annealing was performed in a conventional furnace operated in air.

For the characterization of the thickness of the amorphous layers and the crystallinity of the implanted regions in the as-implanted and annealed samples, respectively, Rutherford backscattering spectrometry measurements in channeling geometry (RBS-C) (Ref. 27) were performed by the use of a 0.9-MeV He^{2+} beam from IONAS.

The TOF-ERDA measurements for depth profiling the Li, ^{16}O, and ^{18}O contents were performed with a 34-MeV $^{127}I^{6+}$ ion beam obtained from the 5-MV EGP-10-II tandem accelerator of the University of Helsinki. The detection angle was 40° relative to the beam direction. The energies of the recoils were obtained from the time-of-flight signals and the energy detector signal was used for mass separation only. The depth distributions were calculated from the energy spectra using the bulk density 2.65 g/cm^2 of SiO_2 and Ziegler-Biersack-Littmark (ZBL) stopping powers for energy loss calculations.[26] The measurement system and depth distribution calculation procedure are discussed in detail in Ref. 28. An unimplanted sample was used for background reduction. In the analysis, the detection efficiency of the two carbon foil timing detectors was taken into account.[29]

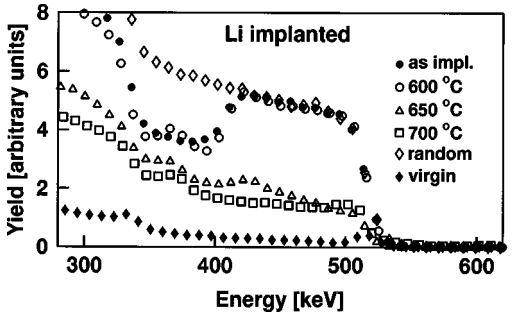

FIG. 1. Channeling RBS spectra of α-quartz implanted with 15-keV Li, taken after 1 h annealings in an ^{18}O atmosphere.

III. RESULTS

A. Li implantation

Figure 1 shows part of the RBS-C spectra of a series of Li-irradiated samples after 1 h thermal annealing at 300–700 °C in the ^{18}O atmosphere. Since the ion fluence was well above the critical value required for amorphizing α-quartz,[30] a 170-nm-thick amorphous layer was formed in the implantation. Up to 600 °C no alteration of the damaged structure was observed, excluding a small shift of the *a*/*c* interface at 600 °C. Significant recrystallization of the amorphous layer started at 650 °C. After annealing at 700 °C, however, no further recrystallization could be observed, indicating that a large amount of stable defects was left. In the sample annealed in air there was about the same amount (25%) of structural damage left. No planar movement of the *a*/*c* interface was observable. Figure 2 illustrates the reduction of the RBS-C yield from the implanted region as a function of the annealing temperature which is a measure of the damage left in the amorphized zone.

Migration of Li atoms in the annealed samples as obtained in the TOF-ERDA measurements is illustrated in Fig. 3(a). The original shape of the Li profile was well preserved in the samples annealed in the ^{18}O atmosphere, whereas in those annealed in air an increase of Li close to the surface (20–70 nm) was observed as illustrated by the 750 °C profile. During the annealing in the ^{18}O atmosphere the loss of Li started at 600 °C. After annealing at 700 °C the maximum

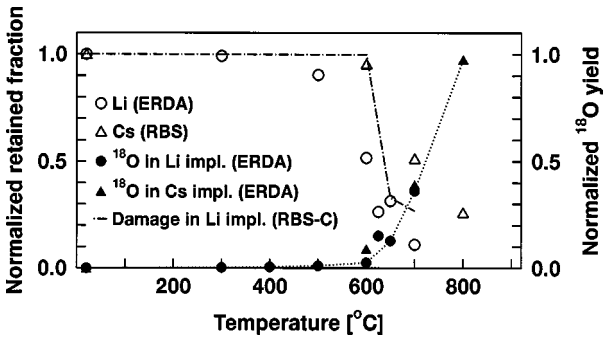

FIG. 2. Loss of the Li and Cs contents (open symbols), increase of the ^{18}O contents (solid symbols), and decrease of the degree of damage (dot-dashed line) in the Li- and Cs-irradiated regions, obtained after annealing the α-quartz samples in the ^{18}O atmosphere. The ^{18}O contents are integrated over the depth from 50 to 170 nm for Li and from 50 to 250 nm for Cs. The dotted line drawn through the ^{18}O points is to guide the eye.

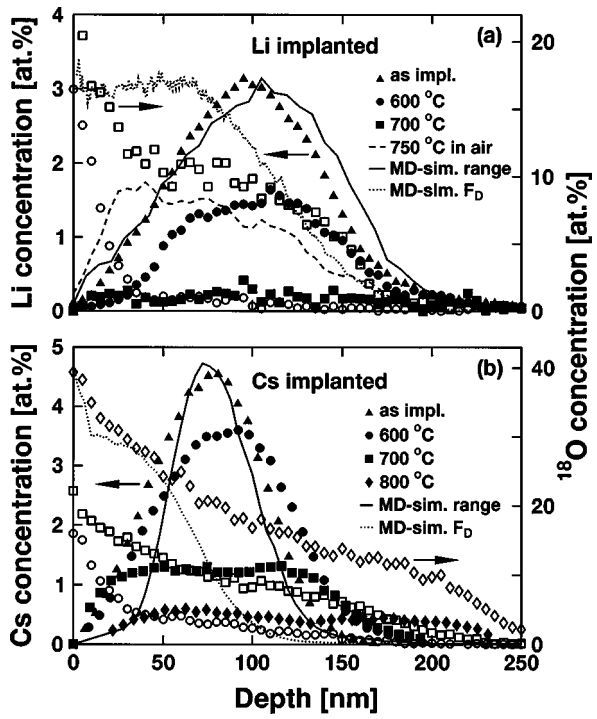

FIG. 3. Concentration distributions of Li (solid symbols) and ^{18}O obtained in TOF-ERDA measurements of the Li-implanted samples annealed in the^{18}O atmosphere. A concentration profile observed after the 750 °C annealing in air is shown for comparison (dashed line). Also shown are the range profile (solid line) and the deposited energy F_D (dotted line) as obtained in the MD calculations. The deposited energy, shown in the figure without *y* scale, has the value of 21 eV/nm/ion at 50 nm. (b) Concentration distributions of Cs (solid symbols) and ^{18}O (open symbols) obtained in RBS and TOF-ERDA measurements of samples implanted with 250-keV Cs ions and annealed in the ^{18}O atmosphere. The MD calculations as for (a). The deposited energy is 140 eV/nm/ion at 50 nm.

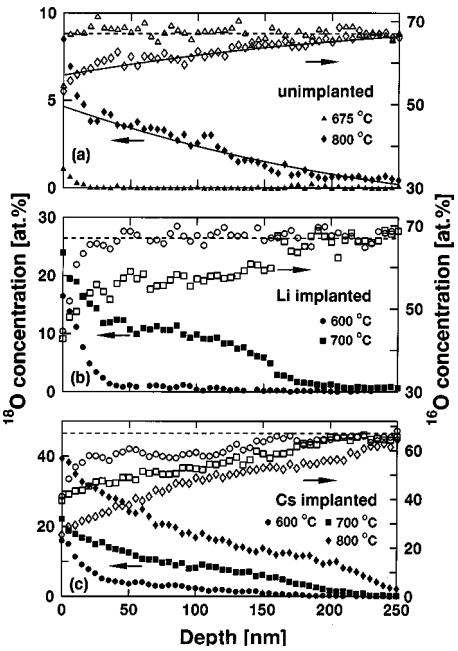

FIG. 4. Concentration distributions of ^{18}O (solid symbols) and ^{16}O (open symbols) obtained in TOF-ERDA measurements of (a) the unimplanted, (b) the 15-keV Li-implanted, and (c) the 250-keV Cs-implanted α-quartz samples annealed in ^{18}O. The solid lines in (a) are the fits used to obtain the diffusitivities of ^{18}O and ^{16}O. The dashed lines shows the stoichiometric ^{16}O concentration of SiO_2.

Li concentration was 0.2 at. % in the implanted region. In the samples annealed in air, the loss of Li was not yet complete at 750 °C; about 50% of the implanted Li atoms was still left with a maximum concentration of 1.8 at. %. The loss of Li in the samples is shown in Fig. 2 as a function of temperature.

TOF-ERDA measurements showed that when annealing the Li-implanted samples in air, the ^{16}O concentration has the constant stoichiometric value of 67 at. %, namely, that of SiO_2. No nitrogen was observed in the ERDA spectra above the 0.1 at. % concentration level. On the other hand, the annealing of nonirradiated α-quartz in the ^{18}O atmosphere at 800 °C led to indiffusion of ^{18}O and outdiffusion of ^{16}O, the total oxygen content having the value of 65 at. % due to the lower intake of ^{18}O than the loss of ^{16}O, Fig. 4(a). The exchange of the oxygen isotopes is peaked towards the surface within the first 25 nm, probably due to defects introduced during grinding and polishing the surface by the manufacturers of α-quartz. By using the analyzing techniques described in Ref. 31, the shapes of the oxygen isotope profiles in the region 250–200 nm resulted in the diffusivity of 7.2 ± 0.3 nm^2/s for ^{16}O and ^{18}O.

Figure 4 summarizes our results concerning the ^{16}O and ^{18}O depth profiles without ion irradiation [Fig. 4(a)], after Li implantation [Fig. 4(b)], and after Cs implantation [Fig. 4(c)]. In the Li-implanted sample the migration of the oxygen isotopes was enhanced, Fig. 4(b). Close to the surface (0–50 nm) there was very much stronger exchange of the oxygen isotopes than in the deeper-lying part of the damaged region from 50 to 200 nm. The ion irradiation enhances the oxygen exchange also with respect to that observed in the grinding and polishing damaged region in the unirradiated samples, Fig. 4(a). At 600 °C the ^{18}O concentration has reached about 1 at. % in the implanted region. A large enhancement can be seen in the 700 °C profile, where the ^{18}O concentration in the modal range region (90–110 nm) of the Li ions is about 11 at. %. Beyond the implanted region of about 200 nm, the ^{18}O concentration is very low. The sum of the ^{18}O and ^{16}O concentrations has the stoichiometric value, independently of the depth. The increase of the total ^{18}O amount in the region 50–200 nm is illustrated in Fig. 2 (solid symbols). The concentration profiles could not be fitted by a function to deduce the diffusivities due to the fact that they are connected to the ion implantation induced damage. In conclusion, the recrystallization of the matrix (Figs. 1 and 2), the loss of Li [Figs. 3(a) and 2], and the take-up of ^{18}O [Fig. 3(a) and Fig. 2] were found to be strongly correlated in a narrow temperature interval between 500 and 700 °C.

B. Cs implantation

Migration of Cs atoms in the samples annealed in the ^{18}O atmosphere, as obtained in the RBS measurements, is illustrated in Fig. 3(b). The boxlike diffusion profiles in these samples are in a good agreement with the results reported earlier for samples annealed in air.[20] The loss of Cs from the samples is included in Fig. 2. The migration was observed to start after annealing at 600 °C without a loss of Cs.

Figure 4(c) shows that in the Cs-implanted samples the exchange of the oxygen isotopes was about the same as in the Li-implanted samples. In the region close to the surface (0–70 nm) the exchange was not as strongly peaked towards the surface as in the Li-implanted samples, the maximum concentrations in the vicinity to the surface being, however, about the same. In the modal range region of the Cs ions (60–100 nm), the ^{18}O concentration varied from about 2 at. % at 600 °C to 10 at. % at 700 °C, both values being about the same as in the Li-implanted samples, and to about 20 at. % at 800 °C. The extensions of the profiles beyond the implantation range of Cs ions (about 150 nm) along with the increasing temperature correlate with the extensions of the Cs profiles; see Fig. 3(b). The total oxygen concentration of about 62 at. % at 600 and 700 °C was below the stoichiometric value in the damaged region and still after the 800 °C annealing slightly below it, namely, about 65 at. %. The increase of the total ^{18}O amount in the 50–250 nm region is illustrated in Fig. 2 and agrees well with that after Li implantation.

The Xe-implanted samples had similar oxygen profiles as the Cs-implanted samples, namely, peaked exchange in the 0–25 nm region and similar ^{16}O and ^{18}O concentrations in the implanted region after annealing at 600 °C. However, no change, excluding an enhanced exchange in the region 0–25 nm, was observed in the concentration distribution after annealing at 700 °C.

The comparison of the Li and Cs profiles with the ^{18}O profiles [see Figs. 3(a) and 3(b)] demonstrates that in the region 0–50 nm the ^{18}O concentrations increased strongly for rising annealing temperature. In the alkali-implanted region the very low ^{18}O concentrations started to increase after the 600 °C annealing when alkali atoms migrated out of the region. The increase is very strong when the alkali concentration is reduced below 0.5 at. %.

The results with both alkali ions are very similar and can be summarized in the following way: (1) After annealing of alkali-implanted α-quartz, recrystallization, alkali migration, and oxygen exchange start at 600 °C. (2) The strong enhancement of the oxygen isotope exchange is accompanied by the complete loss of alkali atoms and recrystallization of the lattice.

IV. DISCUSSION AND CONCLUSIONS

Extended x-ray-absorption fine structure (EXAFS) investigations of ion-irradiated α-quartz have proved that, in spite of the loss of long-range order, the $[SiO_4]$-tetrahedral network remains fully connected, even after high-fluence bombardments.[17] The implantation of alkali ions and annealing in an oxygen-containing atmosphere lead the alkali to act as network modifiers by breaking up the network and generating nonconnected tetrahedron corners.[19,20,22,24] This reduces the average connectivity of the amorphous SiO_2 network and thus increases its recrystallization probability. The importance of alkali network modifiers for the SPEG in α-quartz was demonstrated by Roccaforte *et al.*, who measured an increasing recrystallization rate for increasing Cs concentration, at a constant annealing temperature of 800 °C.[18,22] Disordering of the $[SiO_4]$-tetrahedral network was accompanied by a 20% decrease of the SiO_2 density, indicating a large amount of open volume which can enhance the oxygen migration.

The measured range profiles of Li [Fig. 3(a)] and Cs ions [Fig. 3(b)] were reproduced in molecular dynamics (MD) calculations. The basic algorithms of the simulation code have been discussed in detail elsewhere.[32–34] In short, it is a MD code utilizing domain following and the recoil interaction approximation. The collisions between the ion and the target atoms are treated with pair potentials calculated with the DMol density functional package.[35,36] The electronic slowing down, though small at the energies used, was taken into account as a nonlocal friction force. The electronic stopping power data were taken from Ref. 26. The slowing down was simulated in α-quartz. The comparison of the measured and calculated range profiles is done to confirm the reliability of the calculated deposited energy distributions. The deposited energies are illustrated in Figs. 3(a) and 3(b) for the Li and Cs implantations, respectively. The deposited energy is (at 50 nm) by a factor of 7 higher for the Cs (140 eV/nm/ion) than Li (21 eV/nm/ion) implantations. In the vicinity of the surface a peak of the deposited energy can be observed in both cases.

The exchange between ^{18}O in the annealing atmosphere and ^{16}O in the network has extensively been studied both for crystalline[37] and amorphous SiO_2.[38] For increasing temperature, the increase of thermal vibrations together with the concentration gradient can lead to the incorporation of ^{18}O and outdiffusion of ^{16}O,[39] as obtained also in the current work, Fig. 4(a).

Our data show that in the irradiated region not only the incorporation of ^{18}O but also the damage (deposited energy and implanted atoms) enhances the release of ^{16}O. We attribute the oxygen exchange close to the surface (0–50 nm) observed in all the samples to defects introduced by the grinding and polishing of the sample surfaces and the strong enhancement of the exchange to the deposited energy during ion irradiation.

The comparison of the Li-, Cs-, and Xe-implanted samples in the range region of the implants shows the enhancement of the oxygen exchange and depletion of ^{16}O with respect to the deposited energy and implanted atoms. The similarity of the profiles after the 600 °C annealing in Cs- and Xe-implanted samples is mainly explained by the deposited energy, namely, 140 eV/nm/ion at 50 nm for both the Cs and Xe implantations. The damage due to the immobile implanted atoms can also be expected to affect the profiles. The effect of implanted atoms can clearly be differentiated by comparing the oxygen profiles in the samples after the 700 °C annealing. A strong exchange was observed in the Li- and Cs-implanted samples but not in the Xe-implanted ones. The deposited energy (21 eV/nm/ion at 50 nm) in the Li implantation was not sufficient for the ^{16}O depletion and oxygen exchange related to that, as demonstrated by the oxygen profiles after the 600 °C annealing in Figs. 4(b) and 4(c).

The difference in the Li profiles and contents in the samples annealed in the ^{18}O atmosphere and air [Fig. 3(a)] indicates that an increase of the oxygen content in the annealing atmosphere enhances the Li migration.

The possible formation of alkali-oxide network modifiers has been discussed to be responsible for the modification of the SiO_2 network resulting in SPEG of α-quartz.[20,22] How-

ever, our data do not show evidence for the stoichiometric formation of alkali oxides, as they show a much stronger incorporation of ^{18}O (about two orders of magnitude higher oxygen than the alkali concentration) accompanied by one-to-one exchange with ^{16}O and by SPEG. It is plausible that at 600 °C the dissociation of defect complexes consisting of radiation damage, alkali, and oxygen and the increasing mobilities of these constituents lead to SPEG.

In the annealing of Cs-implanted α-quartz, SPEG starts when the diffusing alkali atoms reach the c/a interface acting as nucleation centers for the planar regrowth. Since Cs is not soluble in the crystalline network, it is driven, along with the moving c/a interface, towards the surface from where it evaporates. An activation energy of 2.83 ± 0.20 eV has been obtained for the recrystallization.[20] In the Li-implanted samples no planar movement of the interface was observed, probably due to the fast outdiffusion. An interpretation of the RBS-C data could be that epitaxial regrowth takes place along columns and a large amount of damage remains.

In the Cs-implanted samples annealed in air, the migration of Cs was concluded to be governed by the Cs dissolution and distribution in SiO_2, Cs reflection at the c/a front, and evaporation from the surface. From the Cs loss an activation energy for this complex process was estimated to be 0.98 ± 0.01 eV.[20] The Cs loss observed in the current work yields an activation energy of 1.2 ± 0.4 eV. The similar values (as well as the similar concentration profiles) indicate that the higher oxygen content in the annealing atmosphere did not enhance the Cs migration. The migration of Li is not connected to the c/a front and the loss is much faster than that of Cs, resulting in an activation energy of 0.45 ± 0.09 eV.

The lower recrystallization temperatures in the case of alkali implantation than in implantation of other atoms, such as self-ions and Xe, can be explained by the fact that Si-O bonds (having the bond energy of 4.57 eV, Ref. 40) are weakened by the presence of alkali atoms, providing alternative bonds for oxygen atoms. The bond energies for Li-O and Cs-O are 3.46 and 3.07 eV, respectively.[41] The lower recrystallization temperature of Li-implanted samples as compared to Cs, is attributed to the higher attraction of Li by the oxygen tetrahedral corners.[42] The weakening of the Si-O bond defines the flexibility of the tetrahedron leading to decrease of the viscosity of the structure and increase of the recrystallization rate.[43] The $^{18}O/^{16}O$ exchange exchange rate is interpreted to qualitatively reflect the number of the Si-O bonds weakened by the mobile alkali atoms.

In conclusion, we have studied epitaxial regrowth of alkali-ion-irradiated, amorphized α-quartz. RBS-C was used to monitor the recrystallization of the implanted region. Recrystallization was completed after 700 °C (Li) or 870 °C (Cs) ^{18}O annealing of the samples. The concentration profiles of the implanted Li and of ^{16}O and ^{18}O, obtained in the TOF-ERDA measurements, and of the implanted Cs obtained via RBS, indicate a dramatic $^{18}O/^{16}O$ exchange between the annealing gas and the amorphized SiO_2 layer, a loss of the implanted alkali atoms, and partial (Li) or full (Cs) SPEG of the damaged region. These results demonstrate that mobile alkali weakens Si-O bonds, enhancing the flexibility of $[SiO_4]$-tetrahedral units and migration of oxygen. Oxygen is trapped at the lattice sites during the recrystallization of α-quartz.

ACKNOWLEDGMENTS

The present work has been funded by Deutsche Forschunggemeinschaft and the Academy of Finland under Projects No. 35073 and No. 44215. We are indebted to D. Purschke and S. Dhar for their efficient help during the ion implantations and channeling measurements and to H. Sepponen during the ERDA measurements. Also thanked are F. Harbsmeier and S. Dhar for fruitful discussions and T. Ahlgren for his valuable aid on diffusion. Juhani Keinonen gratefully acknowledges the Academy of Sciences of Göttingen for financial support and an invitation to visit as Gauss professor.

[1] R.A.B. Devine, Nucl. Instrum. Methods Phys. Res. B **46**, 244 (1990).
[2] C.W. White, J.D. Budai, S.P. Withrow, J.G. Zhu, E. Sonder, R.A. Zuhr, A. Meldrum, D.M. Hembree, D.O. Henderson, and S. Prawer, Nucl. Instrum. Methods Phys. Res. B **141**, 228 (1998).
[3] P.J. Chandler, F.L. Lama, P.D. Townsend, and L. Zhang, Appl. Phys. Lett. **53**, 89 (1988).
[4] P.J. Chandler, L. Zhang, and P.D. Townsend, Nucl. Instrum. Methods Phys. Res. B **46**, 69 (1990).
[5] U. Katenkamp, H. Krage, and R. Prager, Radiat. Eff. **48**, 31 (1980).
[6] M.R. Pascucci, J.L. Hutchinson, and L.W. Hobbs, Radiat. Eff. **74**, 219 (1983).
[7] H. Fischer, G. Götz, and H. Karge, Phys. Status Solidi A **76**, 249 (1983).
[8] H. Beez, D. Fasold, and H. Karge, Phys. Status Solidi A **76**, K171 (1983).
[9] R.G. Macaulay-Newcombe and D.A. Thompson, Nucl. Instrum. Methods Phys. Res. B **1**, 176 (1984).
[10] R.G. Macaulay-Newcombe, D.A. Thompson, J. Davies, and D.V. Stevanovic, Nucl. Instrum. Methods Phys. Res. B **46**, 180 (1990).
[11] H. Fischer, G. Götz, and H. Karge, Phys. Status Solidi A **76**, 493 (1983).
[12] U.B. Ramambaran, H.E. Jackson, and G.C. Farlow, Nucl. Instrum. Methods Phys. Res. B **59/60**, 637 (1991).
[13] G.W. Arnold, Nucl. Instrum. Methods Phys. Res. B **65**, 213 (1992).
[14] F. Harbsmeier, W. Bolse, M.R. da Silva, M.F. da Silva, and J.C. Soares, Nucl. Instrum. Methods Phys. Res. B **136-138**, 263 (1998).
[15] G. Götz, in *Ion Beam Modification of Insulators*, edited by P. Mazzoldi and G.W. Arnold (Elsevier, Amsterdam, The Netherlands, 1987), p. 412.
[16] C.S. Marians and L.W. Hobbs, J. Non-Cryst. Solids **124**, 242 (1990).
[17] W. Bolse, J. Conrad, F. Harbsmeier, M. Borowski,and T. Rödle, Mater. Sci. Forum **248/249**, 319 (1997).

[18] F. Harbsmeier and W. Bolse, Mater. Sci. Forum **248/249**, 279 (1997).
[19] W. Bolse, Nucl. Instrum. Methods Phys. Res. B **141**, 133 (1998).
[20] F. Roccaforte, W. Bolse, and K.P. Lieb, Appl. Phys. Lett. **73**, 1349 (1998).
[21] F. Roccaforte, W. Bolse, and K.P. Lieb, Appl. Phys. Lett. **74**, 1922 (1999).
[22] F. Roccaforte, W. Bolse, and K.P. Lieb, Nucl. Instrum. Methods Phys. Res. B **148**, 692 (1999).
[23] W. Bolse, Nucl. Instrum. Methods Phys. Res. B **148**, 83 (1999).
[24] G.W. Arnold and P. Mazzoldi, in *Ion Beam Modification of Insulators*, edited by P. Mazzoldi and G.W. Arnold (Elsevier, Amsterdam, The Netherlands, 1987), p. 192.
[25] M. Uhrmacher, K. Pampus, F.J. Bergmeister, D. Purschke, and K.P. Lieb, Nucl. Instrum. Methods Phys. Res. B **9**, 234 (1985).
[26] J.F. Ziegler and J.P. Biersack, computer code TRIM95, version 95.9.
[27] W.K. Chu, J.W. Meyer, and M.-A. Nicolet, *Backscattering Spectrometry* (Academic Press, Orlando, FL, 1978).
[28] J. Jokinen, J. Keinonen, P. Tikkanen, A. Kuronen, T. Ahlgren, and K. Nordlund, Nucl. Instrum. Methods Phys. Res. B **119**, 533 (1996).
[29] T. Sajavaara, J. Jokinen, K. Arstila, and J. Keinonen, Nucl. Instrum. Methods Phys. Res. B **139**, 225 (1998).
[30] F. Harbsmeier and W. Bolse, J. Appl. Phys. **83**, 4049 (1998).
[31] E. Vainonen, J. Likonen, T. Ahlgren, P. Haussalo, J. Keinonen, and C.H. Wu, J. Appl. Phys. **82**, 3791 (1997).
[32] K. Nordlund, Comput. Mater. Sci. **3**, 448 (1995).
[33] J. Keinonen, A. Kuronen, K. Nordlund, R.M. Nieminen, and A.P. Seitsonen, Nucl. Instrum. Methods Phys. Res. B **88**, 382 (1994).
[34] K. Nordlund and A. Kuronen, Nucl. Instrum. Methods Phys. Res. B **115**, 528 (1996).
[35] J. Delley, J. Chem. Phys. **92**, 508 (1990).
[36] DMol is a trademark of Bio Sym. Inc., San Diego, CA.
[37] B.J. Giletti and R.A. Yund, J. Geophys. Res. **89**, 4039 (1984).
[38] A.G. Revesz, B.J. Mnstik, and H.L. Hughes, J. Electrochem. Soc. **134**, 2911 (1987).
[39] E.W. Sucov, J. Am. Ceram. Soc. **46**, 14 (1963).
[40] M.A. Lamkin, F.L. Riley, and R.J. Fordham, J. Eur. Ceram. Soc. **10**, 347 (1992).
[41] J.B. Pedley and E.M. Marshall, J. Phys. Chem. Ref. Data **12**, 967 (1984).
[42] H. Scholze and N.J. Kreoll, *Glass Science and Technology* (Academic Press, London, 1986).
[43] S.X. Weng, L.M. Weng, R.C. Erwing, and R.H. Dorennus, J. Non-Cryst. Solids **238**, 198 (1998).